

MOLECULAR DYNAMICS STUDY OF TEMPERATURE-INDUCED STRUCTURAL CHANGES IN $\text{YBa}_2\text{Cu}_3\text{O}_7$ CRYSTAL

JAROSŁAW BOŚKO AND WOJCIECH SADOWSKI

*Department of Solid State Physics,
Faculty of Technical Physics and Applied Mathematics,
Technical University of Gdansk,
Narutowicza 11/12, 80–952 Gdansk, Poland*

Abstract: The structure of $\text{YBa}_2\text{Cu}_3\text{O}_7$ crystal has been studied with the aid of molecular-dynamics (MD) technique. Two-body model potentials proposed by Zhang and Catlow have been used in MD simulations performed in a wide range of temperatures. The temperature-induced orthorhombic-to-tetragonal phase transition is observed. The destruction of the arrangement of atoms in the CuO chains due to diffusion of oxygen atoms is observed. The diffusion coefficients are calculated, and their variation as a function of temperature is analysed. The activation energy is estimated.

Keywords: MD simulation, structure, phase transition, oxygen diffusion, trajectory

1. Introduction

$\text{YBa}_2\text{Cu}_3\text{O}_{7-\delta}$ crystal (Figure 1) is one of the high temperature superconducting cuprates. The common feature of this family of materials is their layered structure [1]. In the case of $\text{YBa}_2\text{Cu}_3\text{O}_{7-\delta}$ crystal (YBCO) one can distinguish the CuO_2 sheets ($\text{Cu}(2),\text{O}(2,3)$). The mobile charge carriers (holes) responsible for the superconducting properties are localised in these sheets. In the structure there are also the CuO planes with the $\text{Cu}(1)$ and $\text{O}(1)$ ions arranged in the chains. These serve as charge reservoirs.

Although there is no simple relationship between the structure of the crystal and its superconducting transition temperature, the various correlations have been observed and reported in the literature. For example, the dependence of the T_C on some atom-atom distances in the different cuprates was studied [1, 2]. Also the oxygen stoichiometry and ordering play a crucial role in determining the properties of the YBCO crystal. It is known that the critical temperature T_C depends on the value of δ . The material is superconducting when it is as much oxygenated as possible ($T_C = 90$ K is obtained for $\delta \sim 0$, the maximal $T_C = 92$ K is obtained for $\delta \sim 0.05$), and the additional oxygen atoms are arranged and form CuO chains.

In the present paper the structure of the $\text{YBa}_2\text{Cu}_3\text{O}_7$ crystal is studied with the

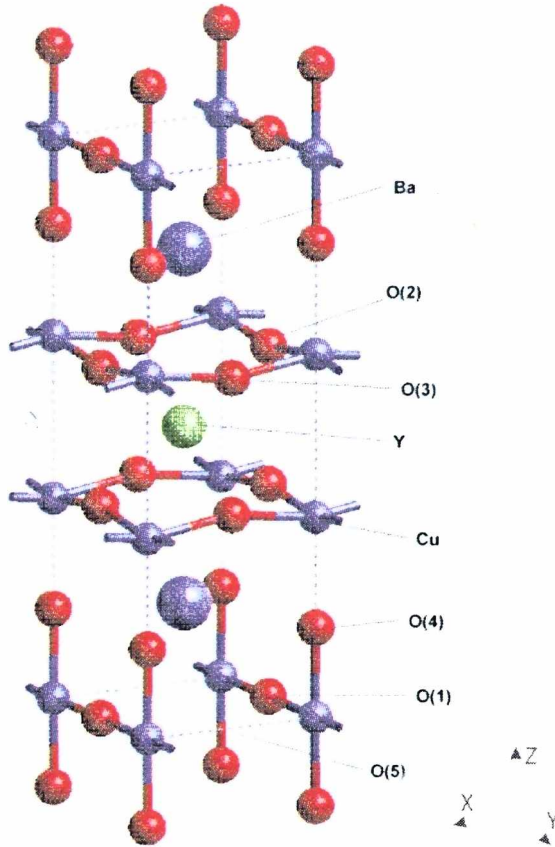


Figure 1. Structure of $YBa_2Cu_3O_7$.

aid of the molecular–dynamics (MD) method. The model and the simulation parameters are described in the next chapter. This is followed by the simulation results. In subsequent sections the equilibrium structure, the temperature–induced structural changes of the material, and finally the results of the study of the oxygen atoms diffusion are presented.

2. Simulation method

As a tool in our study the atomistic simulation method has been chosen. The method accuracy is determined by the quality of the interatomic potentials describing the system, and the assignment of charges to each ion in the solid. In our model charge states of 3+, 2+ and 2+ were assigned to Y, Cu and Ba ions, respectively. To achieve electroneutrality, all O ions, except for those in CuO chains, were given the charge of 2-. The O anions in chains have the charge of 1-. The system was treated as an assembly of rigid ions. Interatomic potentials were separated into Coulombic, and short–range terms. The long–range Coulomb interactions were handled using the Ewald technique. The short–range potentials were of the two–body Buckingham form:

$$\phi_{ij} = A \cdot \exp(-r/\rho) - C/r^6. \quad (1)$$

The potential parameters proposed by Zhang and Catlow [3] were used in our study (Table 1).

The simulations were performed using a box containing 975 atoms, which corresponded to 75 crystal unit cells. The system remained in the isothermal-isobaric regime with the Nose'-Hoover thermostat. The equations of motion were integrated with a 1 fs time step. Initially, a Maxwell-Boltzmann distribution of velocities was assigned to all the atoms in the simulation box. Iterative velocity scaling was employed to achieve a stable temperature. The system was then allowed to equilibrate for 100 ps to produce the trajectories, which were analysed.

The calculations were performed on the SGI Power Challenge 8×R10000 computer using the MOLDY computer code.

Table 1. Potential parameters for short-range interactions

	A (eV)	ρ (Å)	C (eV·Å ⁶)
O ²⁻ -O ²⁻	22764.3	0.14900	25.0
O ²⁻ -O ¹⁻	22764.3	0.14900	25.0
O ²⁻ -Cu ²⁺	3799.3	0.24273	0.0
O ²⁻ -Ba ²⁺	3115.5	0.33583	0.0
O ²⁻ -Y ³⁺	20717.5	0.24203	0.0
O ¹⁻ -O ¹⁻	22764.3	0.14900	25.0
O ¹⁻ -Cu ²⁺	1861.6	0.25263	0.0
O ¹⁻ -Ba ²⁺	29906.5	0.27238	0.0
Cu ²⁺ -Ba ²⁺	168128.6	0.22873	0.0
Ba ²⁺ -Ba ²⁺	2663.7	0.25580	0.0

3. Simulation results

3.1. Equilibrium structure

The potential applied in our model reproduces the structure of YBCO with a maximum error in the most structural parameters of 3.5 % (see Table 2). The simulation was performed in the constant temperature $T = 300$ K. The bond lengths were estimated from the radial distribution functions. The essential feature of the

crystal is its anisotropy and layered structure. The bond lengths obtained with lower accuracy correspond to the distances between those layers. Within the layers the bond lengths are in a good agreement with the experimentally observed values [4].

Table 2. The comparison of the calculated and experimental lattice constants and bond lengths

Bond	Experimental length (Å)	Calculated length (Å)	Difference (Å)	Differences (%)
<i>a</i>	3.820	3.838	0.018	0.5
<i>b</i>	3.885	3.906	0.021	0.5
<i>c</i>	11.683	12.827	1.144	9.8
Y - O(2)	2.418	2.389	0.029	1.2
Y - O(3)	2.399	2.389	0.010	0.4
Ba - O(1)	2.891	3.235	0.344	11.9
Ba - O(2)	2.980	3.050	0.070	2.3
Ba - O(3)	2.948	3.050	0.102	3.5
Ba - O(4)	2.750	2.843	0.093	3.4
Cu(1) - O(1)	1.947	1.945	0.002	0.1
Cu(1) - O(4)	1.834	1.815	0.019	1.0
Cu(2) - O(2)	1.929	1.941	0.012	0.6
Cu(2) - O(3)	1.961	1.941	0.020	1.0
Cu(2) - O(4)	2.341	2.921	0.580	24.8

3.2. The temperature-induced structural changes

A series of simulations was performed for the system held in the temperature varying from 300 K up to 1500 K. Figure 2a shows how the calculated lattice parameters *a* and *b* vary as a function of temperature. They expand linearly up to 700 K. Above this value, the *a* axis expands much faster, and finally the *a* and *b* axes become equal, and the crystal becomes tetragonal. The temperature at which the orthorhombic-to-tetragonal transition occurs amounts approximately to 900 K. This phase transition was observed experimentally [5] and the variation of the lattice constants as a function of temperature is presented in Figure 2b. It occurs due to the diffusion of the oxygen ions. Moreover, above 700K the oxygen loss takes place. In our model the number of atoms is conserved, so the structural changes are caused only by the redistribution of vacancies over O(1), O(4) and O(5) sites. Because of the constant stoichiometry, the simulated crystal corresponds to the one held in a high oxygen partial pressure. The temperature at which the transition occurs for the oxygen pressure equal 1 atm is 950 K [4]. It is in good agreement with the value obtained in our calculation.

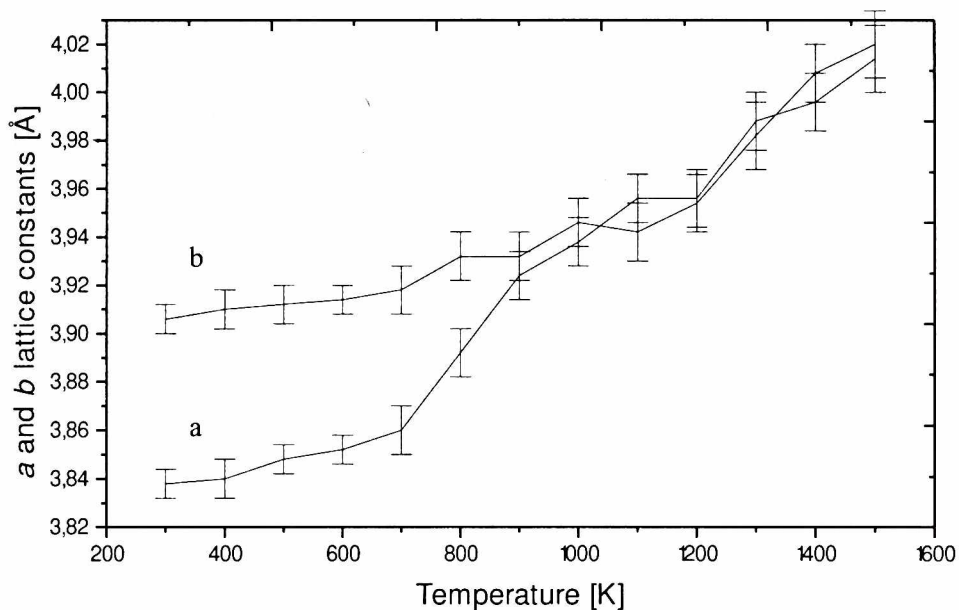


Figure 2a. The lattice constants a and b versus temperature

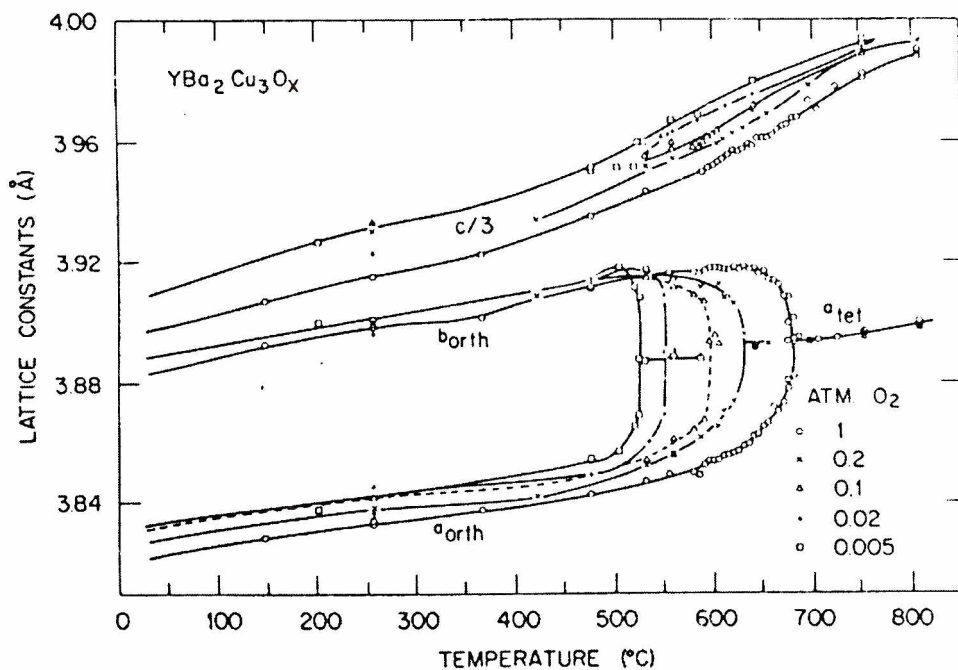


Figure 2b. Experimentally observed variation of the lattice constants versus temperature for various oxygen partial pressure [5]

3.3. The diffusion of the oxygen atoms

Since the observed structural phase transition of the crystal occurs due to the diffusion and the redistribution of the oxygen ions within the crystal, we studied the recorded trajectories, paying special attention to the temperature-activated migration of oxygen. The mean square displacement (MSD) of the oxygen atoms as a function of time was calculated. A plot of MSD against time enables the diffusion coefficient to be calculated from the gradient using the Einstein relation [6]:

$$\langle |r(t) - r(0)|^2 \rangle = B + 6D \cdot t, \quad (2)$$

where $|r(t) - r(0)|$ is the displacement of a particle from its initial position. These are averaged over the particles concerned and over time. D is the diffusion coefficient of oxygen, and B is the thermal factor arising from atomic vibrations. Figure 3 shows the MSD plot for the oxygen atoms at $T = 1200\text{K}$. The obtained oxygen diffusion coefficients at different temperatures are presented in Table 3.

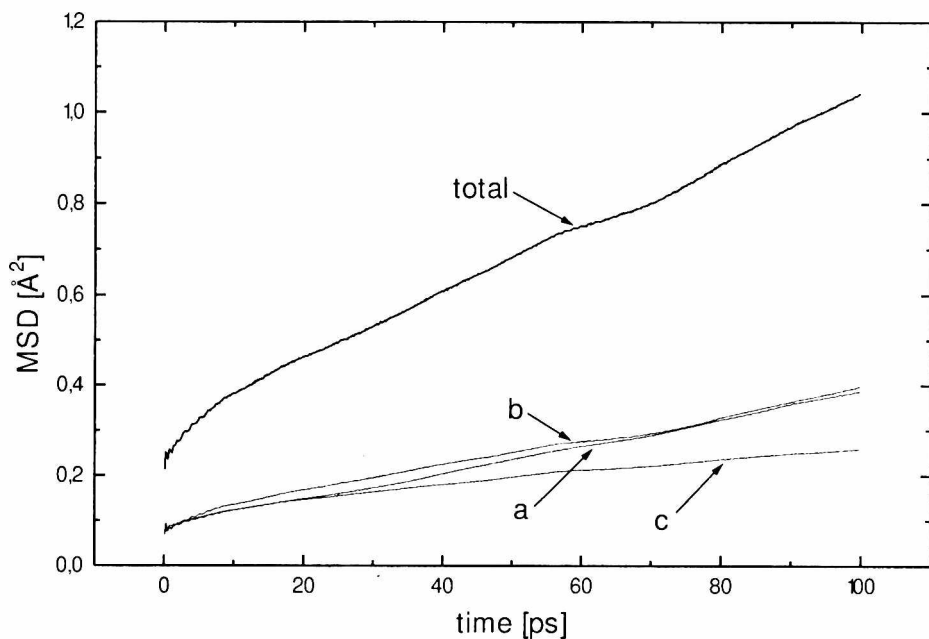


Figure 3. MSD plot versus time at $T = 1300\text{K}$. Curves a, b, c and total correspond to the MSD in the a, b and c directions, respectively, and to the total MSD

Table 3. The calculated diffusion coefficients in the a , b , c directions, and the total one

T (K)	D_a (10^{-12} m ² /s)	D_b (10^{-12} m ² /s)	D_c (10^{-12} m ² /s)	D (10^{-12} m ² /s)
1100	17.8599	18.5803	13.0544	51.0134
1200	30.1706	27.3782	14.2078	71.4963
1300	35.7982	26.6827	40.2736	106.2506
1400	73.2522	38.3071	21.3781	135.2210

The coefficients for diffusion in the a and b directions (D_a and D_b respectively) are similar and in most cases greater than coefficient for the c direction (D_c); D_a in high temperature is larger than D_b . The oxygen diffusion is associated with the jumps of the atoms to the vacant sites in the crystal structure. In the YBCO crystal there are four different sites which can be occupied by the oxygen atoms (see Figure 1). These are as follows:

1. O(2) and O(3) sites which form CuO_2 planes. Atoms which occupy these sites do not diffuse until the crystal is melted.
2. O(4) apical sites. At high temperature atoms jump from these sites to the vacancies in the CuO planes; they contribute to the diffusion in the c direction. In this way the vacancies in the apical sites are formed.
3. O(1) sites. At room temperature all are occupied and form the CuO chains, at higher temperature they are redistributed over the vacant O(4) and O(5) sites.
4. O(5) sites. At room temperature all are unoccupied. Above the temperature of the orthorhombic-to-tetragonal transition are occupied either by the O(1) or O(4) atoms.

Analysis of the particle trajectories obtained in the simulations allowed us to observe the migration mechanisms and jumps of atoms between the particular sites. In Figures 4 and 5 there are presented the trajectories of the oxygen atoms within the crystal. Also the copper atoms are shown (green colour in the picture); these only vibrate near their equilibrium positions. Figure 4 shows the plane, which contains the CuO chains. One can see the jumps of the oxygen atoms between the O(1) and O(5) sites. In Figure 5 the plane along the b and c directions is presented. In this case one can observe the migration of atoms between the O(1) and O(5) sites. In this picture neither the O(2) nor O(3) atoms are shown; these ones do not diffuse and only vibrate at the equilibrium sites.

The diffusion is thermally activated and the diffusion coefficient is supposed to depend on the temperature according to the following equation:

$$D = D_0 \exp\left(-\frac{E_a}{k_B T}\right), \quad (3)$$

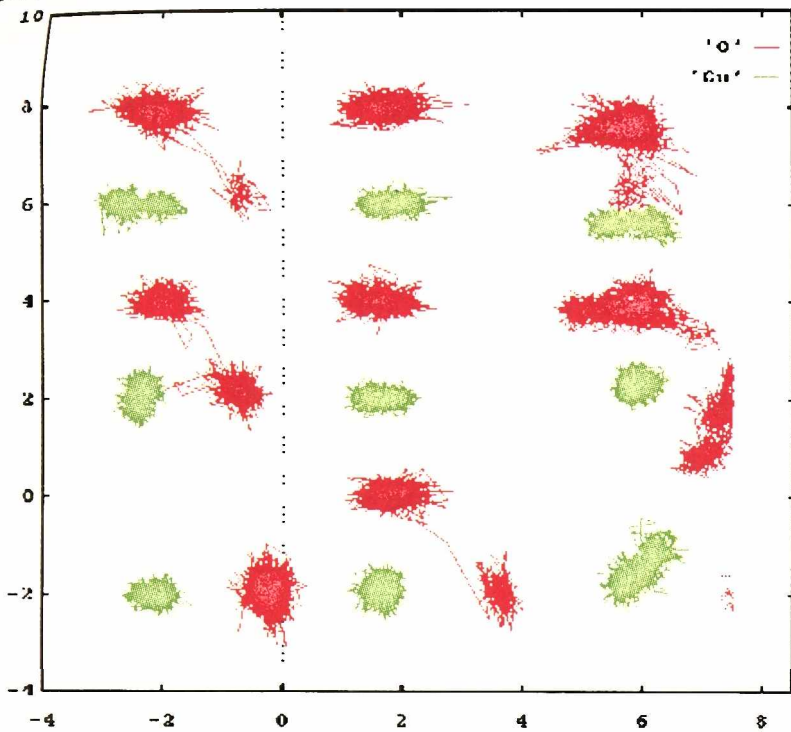


Figure 4. The xy projection of the trajectories of the oxygen (red) and copper (green) atoms in the CuO plane at 1200 K for a duration of 100 ps (in Å)

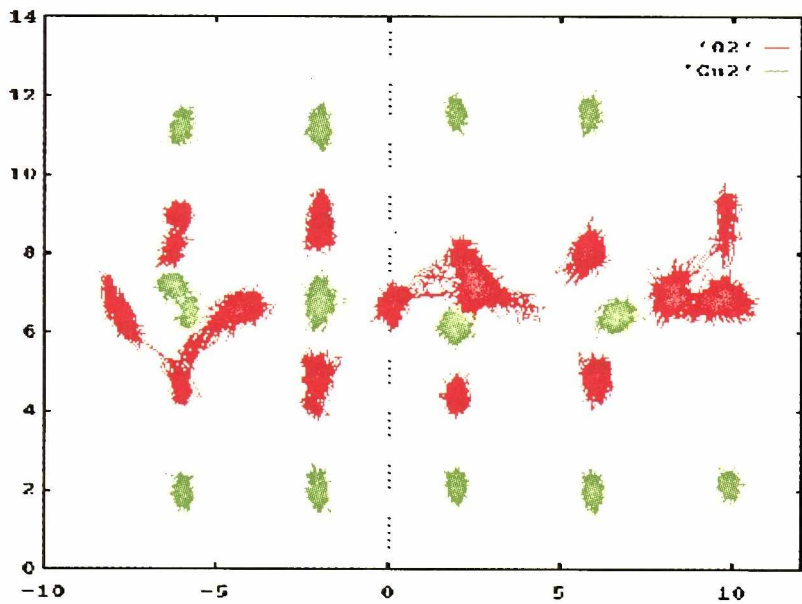


Figure 5. The yz projection of the trajectories of the oxygen (red) and copper (green) atoms at 1200 K for a duration of 100 ps (in Å)

where E_a is an activation energy. From the Arrhenius plot $\ln(D)$ vs $1000/T$ we estimated the value of E_a . The plot is presented in Figure 5 and the obtained constants are as follows: $E_a = 0.44$ eV and $D_0 = 5.27 \cdot 10^{-9} \text{ m}^2\text{s}^{-1}$.

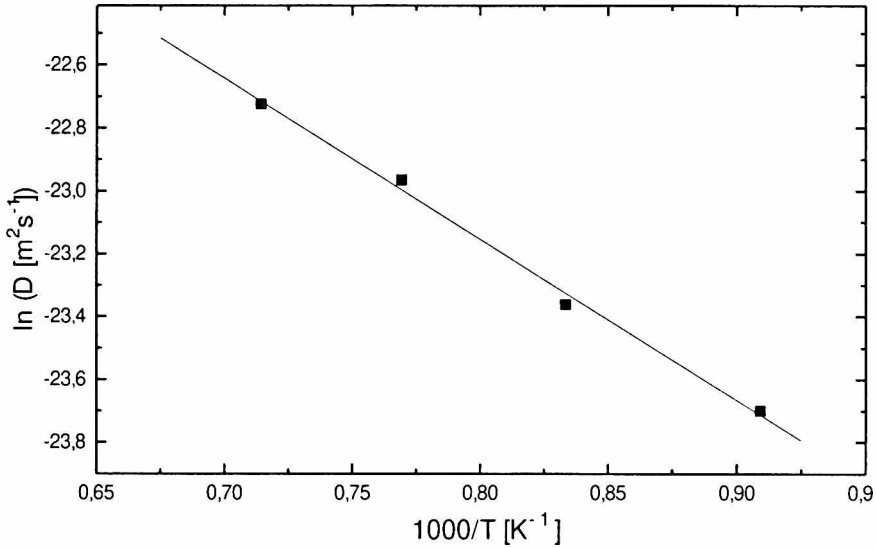


Figure 6. Arrhenius plot $\ln(D)$ vs $1000/T$

From the experimental data [7] the expression for the diffusion coefficient was derived and has the form:

$$D = 1.4 \cdot 10^{-8} \exp\left(-\frac{0.98 \text{ eV}}{k_B T}\right) \text{ m}^2 \text{ s}^{-1} \quad (4)$$

The values obtained in the simulation are rather in a poor agreement with the experimental ones. The activation energy is smaller than the one obtained from the experimental data, and it could be due to the weaker interaction between the layers of the crystal. As noted above, the structure of the crystal was reproduced in good agreement with the experimentally observed one except for the distances between the layers (CuO, Ba and CuO₂ planes). Larger distances lead to weaker bonding of ions and less energy is needed to activate their migration through the crystal. Also is smaller than the one estimated from the experiment. In the samples, which are studied experimentally there is always a number of oxygen vacancies, which are distributed over the O(1) sites ($\delta > 0$). The difference in the stoichiometry (in comparison to the modelled $YBa_2Cu_3O_7$ crystal) could be responsible for the difference in the value of D_0 .

4. Conclusions

In our study of the YBCO crystal we employed the molecular dynamics technique. The advantages and disadvantages of the two-body interaction potential parameterised by Zhang and Catlow have been analysed. The structure of the

crystal obtained in the simulation was in good agreement with the experimental data. The simulations were performed in a wide range of temperatures (300–1500 K) and the structural orthorhombic-to-tetragonal phase transition was observed. The migration of the oxygen atoms and their redistribution within the crystal was found to be responsible for this transition. The possible oxygen jump paths observed in the simulation are as follows: O(1)–O(5), O(1)–O(4), and O(4)–O(5). The diffusion coefficients at different temperatures and in different directions were calculated. The values of D_a and D_b are comparable and both are larger than D_c . These results can be explained in terms of the recorded oxygen atom jumps. The calculated diffusion coefficients and the estimated activation energy are rather in a poor quantitative agreement with the experimental ones. It is due to the potential parameters, which wrongfully reproduce the interlayer distances. Probably more reliable results could be obtained if a better set of potential parameters was used. Such work, based on the ab initio calculations, is in progress.

Acknowledgements

The opportunity to perform our numerical calculations at the TASK Computer Centre (Gdansk, Poland) is kindly acknowledged.

References

- [1] Rao C N R and Ganguli A K 1995 *Chem. Soc. Rev.* 1
- [2] Jorgensen J. D., Veal B. W., Paulikas A. P., Nowicki L. J., Crabtree G. W., Claus H. and Kwok W. K. 1990 *Phys. Rev.* **B 41** 1863
- [3] Zhang X and Catlow C R A 1992 *Phys. Rev.* **B 46** 457
- [4] Beyers R and Shaw T M *Solid State Physics* **42** 135
- [5] Specht E. D., Sparks C. J., Ghore A. G., Brynestad J., Cavin O. B., Kroeger D. M. and Oye H. A. 1988 *Phys. Rev.* **B 37** 7426
- [6] Allen M P and Tildesley D J *Computer simulation of liquids*, Clarendon Press, Oxford, 1987
- [7] Rothman S J, Routbort J L and Barker J E 1989 *Phys. Rev.* **B 40** 8852